IFUM-911-FT
Edinburgh 2008/1
CERN-PH-TH/2008-009

Higgs production via gluon-gluon fusion with finite top mass beyond next-to-leading order

Simone Marzani,[a], Richard D. Ball,[a,b] Vittorio Del Duca,[c1]
Stefano Forte[d] and Alessandro Vicini[d]

[a] *School of Physics, University of Edinburgh, Edinburgh EH9 3JZ, Scotland, UK*

[b] *CERN, Physics Department, Theory Division, CH-1211 Genève 23, Switzerland*

[c] *INFN, Laboratori Nazionali di Frascati, Via E. Fermi 40, I-00044 Frascati, Italy*

[d] *Dipartimento di Fisica, Università di Milano and INFN, Sezione di Milano, Via Celoria 16, I-20133 Milano, Italy*

Abstract

We present a computation of the cross section for inclusive Higgs production in gluon–gluon fusion for finite values of the top mass in perturbative QCD to all orders in the limit of high partonic center–of–mass energy. We show that at NLO the high energy contribution accounts for most of the difference between the result found with finite top mass and that obtained in the limit $m_t \to \infty$. We use our result to improve the known NNLO order result obtained at $m_t \to \infty$. We estimate the effect of the high energy NNLO m_t dependence on the K factor to be of the order of a few per cent.

CERN-PH-TH/2008-009
January 2008

[1] On leave from INFN, Sezione di Torino, Italy

1 The cross section in the soft limit and in the hard limit

The determination of higher–order corrections to collider processes [1], and specifically Higgs production [2] in perturbative QCD is becoming increasingly important in view of forthcoming phenomenology at the LHC. The dominant Higgs production mechanism in the standard model is inclusive gluon–gluon fusion ($gg \to H + X$) through a top loop. The next–to–leading order corrections to this process were computed several years ago [3, 4] and turn out to be very large (of order 100%). The bulk of this large correction comes from the radiation of soft and collinear gluons [5], which give the leading contribution in the soft limit in which the partonic center-of-mass energy $\hat{s}$ tends to the Higgs mass m_H^2, and which at LHC energies turns out to dominate the hadronic cross section after convolution with the parton distributions.

This dominant contribution does not resolve the effective gluon-gluon-higgs (ggH) coupling induced by the top loop. As a consequence, the NLO correction can be calculated [6, 7] quite accurately in the limit $m_t \to \infty$, where it simplifies considerably because the ggH coupling becomes pointlike and the corresponding Feynman diagrams have one less loop. Recently, the NNLO corrections to this process have been computed in the $m_t \to \infty$ limit [8]. The NNLO result appears to be perturbatively quite stable, and this stability is confirmed upon inclusion [9] of terms in the next few orders which are logarithmically enhanced as $\hat{s} \to m_H$, which can be determined [10] using soft resummation methods. This suggests that also at NNLO the large m_t approximation should provide a good approximation to the yet unknown exact result.

However, this is only true for the total inclusive cross section: for example, if one looks at the production of Higgs plus jets, if the transverse momentum is large the infinite m_t approximation fails [11]. Indeed, even though the m_t–independent contribution from soft and collinear radiation turns out to dominate the cross section at the hadronic level, it does not necessarily provide a good approximation to the partonic cross section in a fixed kinematical region. In particular, the infinite m_t approximation, which becomes exact in the soft limit, fails in the opposite (hard) limit of large center–of–mass energy. This is due to the fact that the ggH vertex is pointlike in the infinite m_t limit, whereas for finite m_t the quark loop provides a form factor (as we shall see explicitly below). Clearly, a point–like interaction has a completely different high energy behaviour than a resolved interaction which is softened by a form factor: in fact one can show [12] that a point–like interaction at n–th perturbative order has double energy logs while a resolved interaction has only single logs.

This means that as $\hat{s} \to \infty$ the $gg \to H + X$ partonic cross section $\hat{\sigma}$ behaves as

$$\hat{\sigma} \underset{\hat{s}\to\infty}{\sim} \begin{cases} \sum_{k=1}^{\infty} \alpha_s^k \ln^{2k-1}\left(\frac{\hat{s}}{m_H^2}\right) & \text{pointlike: } m_t \to \infty \\ \\ \sum_{k=1}^{\infty} \alpha_s^k \ln^{k-1}\left(\frac{\hat{s}}{m_H^2}\right) & \text{resolved: finite } m_t \end{cases} \tag{1}$$

Hence, as the center-of-mass energy grows, eventually $m_t \to \infty$ ceases to be a good approximation to the exact result. It is clear from eq. (1) that this high energy deviation between the exact and approximate behaviour is stronger at higher orders, so one might expect the relative accuracy of the infinite m_t approximation to the k–th order perturbative contribution to the cross section to become worse as the perturbative order increases. Conversely, this suggests that

it might be worth determining the high energy behaviour of the exact cross section and use the result to improve the infinite m_t result, which is much less difficult to determine. Eventually, a full resummation of these contributions might also become relevant.

The leading high energy contributions to this process in the infinite m_t limit have in fact been computed some time ago in Ref. [13]: this amounts to a determination of the coefficient of the double logs eq. (1), in the pointlike case. In this paper, we compute the coefficients of the single logs eq. (1) in the resolved (exact) case. Our result takes the form of a double integral, whose numerical evaluation order by order in a Taylor expansion gives the coefficient of the logs eq. (1) (at the lowest perturbative order the integral can be computed in closed form). After checking our result against the known full NLO result of Ref. [3, 4], we will discuss the way knowledge of the exact high energy behaviour of the cross section at a given order can be used to improve the infinite m_t result, using the NLO case, where everything is known, as a testing ground. We will show that in fact, at NLO the different high energy behaviour eq. (1) accounts for most of the difference between the exact and infinite m_t cross sections. We will then repeat this analysis in the NNLO case, where only the infinite m_t result is currently known. We will show that in fact at this order the contribution of the logarithmically enhanced terms which dominate the partonic cross section at high energy is substantial even for moderate values of the partonic center-of-mass energy, such as $\hat{s} \sim 2m_H^2$.

The calculation of the leading high energy logs is presented in section 2, while in section 3 we discuss its use to improve the NLO and NNLO results. The appendix collects the explicit expressions of the form factors which parametrize the amplitude for the process $gg \to H$ with two off–shell gluons, which is required for the calculation of sect. 2.

2 Determination of the leading high energy logarithms

2.1 Definitions, kinematics and computational procedure

We compute the total inclusive partonic cross section $\hat{\sigma}(gg \to H + X)$ in an expansion in power of α_s, as a function of the partonic center-of-mass energy $\hat{s}$:

$$\hat{\sigma}(gg \to H + X) = \hat{\sigma}_{gg}\left(\alpha_s; \tau; y_t, m_H^2\right), \tag{2}$$

where the dimensionless variables τ and y_t parametrize respectively the partonic center-of-mass energy and the dependence on the top mass:

$$\tau \equiv \frac{m_H^2}{\hat{s}} \tag{3}$$

$$y_t \equiv \frac{m_t^2}{m_H^2}. \tag{4}$$

The corresponding contribution to the hadronic cross section σ can be obtained by convolution with the gluon-gluon parton luminosity $\mathcal{L}$:

$$\sigma_{gg}(\tau_h; y_t, m_H^2) = \int_{\tau_h}^1 dw\, \hat{\sigma}_{gg}\left(\alpha_s; \frac{\tau_h}{w}; y_t, m_H^2\right) \mathcal{L}(w) \tag{5}$$

$$\mathcal{L}(w) \equiv \int_w^1 \frac{dx_2}{x_2}\, g_{h_1}\left(\frac{w}{x_2}, m_H^2\right) g_{h_2}\left(x_2, m_H^2\right), \tag{6}$$

where $g_{h_i}(x_i, Q^2)$ is the gluon distribution in the i-th incoming hadron and in eq. (5) the dimensionless variables τ_h parametrizes the hadronic center-of-mass energy s

$$\tau_h \equiv \frac{m_H^2}{s}. \tag{7}$$

Note that $0 \le \tau_h \le \tau \le 1$, and that if $y_t < \frac{1}{4}$ then the intermediate $t\bar{t}$ pair produced by the gluon-gluon fusion can go on shell.

It is convenient to define a dimensionless hard coefficient function $C(\alpha_s(m_H^2); \tau, y_t)$

$$\hat{\sigma}_{gg}\left(\alpha_s; \tau; y_t, m_H^2\right) = \sigma_0(y_t) C(\alpha_s(m_H^2), \tau, y_t) \tag{8}$$

$$C(\alpha_s(m_H^2), \tau, y_t) = \delta(1-\tau) + \frac{\alpha_s(m_H^2)}{\pi} C^{(1)}(\tau, y_t) + \left(\frac{\alpha_s(m_H^2)}{\pi}\right)^2 C^{(2)}(\tau, y_t), \tag{9}$$

where $\sigma_0 \delta(1-\tau)$ is the leading order cross section, determined long ago in ref. [14]:

$$\sigma_0(y_t) = \frac{\alpha_s^2 G_F \sqrt{2}}{256\pi} \left| 4 y_t \left(1 - \frac{1}{4}(1-4y_t) s_0^2(y_t)\right)\right|^2, \tag{10}$$

where

$$s_0(y_t) = \begin{cases} \ln\left(\frac{1-\sqrt{1-4y_t}}{1+\sqrt{1-4y_t}}\right) + \pi\, i & \text{if} \quad y_t < \frac{1}{4} \\ 2\, i \tan^{-1}\left(\sqrt{\frac{1}{4y_t - 1}}\right) = 2\, i \sin^{-1}\left(\sqrt{\frac{1}{4y_t}}\right) & \text{if} \quad y_t \ge \frac{1}{4}. \end{cases} \tag{11}$$

We also define the Mellin transform

$$C(\alpha_s(m_H^2), N, y_t) = \int_0^1 d\tau\, \tau^{N-1} C(\alpha_s(m_H^2), \tau, y_t), \tag{12}$$

denoted with the same symbol by slight abuse of notation.

We are interested in the determination of the leading high energy contributions to the partonic cross section $\hat{\sigma}(gg \to H + X)$, namely, the leading contributions to $C(\alpha_s(m_H^2), \tau, y_t)$ as $\tau \to 0$ to all orders in $\alpha_s(m_H^2)$. Order by order in $\alpha_s(m_H^2)$, these correspond to the highest rightmost pole in N in the expansion in powers of $\alpha_s(m_H^2)$ of $C(\alpha_s(m_H^2), N, y_t)$. The leading singular contributions to the partonic cross section $\hat{\sigma}(gg \to H + X)$ to all orders can be extracted [12] from the computation of the cross section for a slightly different process, namely, the cross section $\sigma_{\rm off}(gg \to H)$ computed at leading order, but with incoming off-shell gluons, a suitable choice of kinematics and a suitable prescription for the sum over polarizations.

The procedure used for this determination is based on the so-called high energy (or k_t) factorization [12], and consists of the following steps.

- One computes the matrix element $\mathcal{M}^{\mu\nu}_{ab}(k_1,k_2)$ for the leading-order process $gg \to H$ at leading order with two incoming off-shell gluons with polarization indices μ,ν and color indices a,b. The momenta k_1, k_2 of the gluons in the center-of-mass frame of the hadronic collision admit the Sudakov decomposition at high energy

$$k_i = z_i p_i + \mathbf{k}_i, \tag{13}$$

where p_i are lightlike vectors such that $p_1 \cdot p_2 \neq 0$, and $\mathbf{k}_i$ are transverse vectors, $\mathbf{k}_i \cdot p_j = 0$ for all i,j. The gluons have virtualities

$$k_i^2 = \mathbf{k}_i^2 = -|\mathbf{k}_i|^2. \tag{14}$$

The cross section $\sigma_{\rm off}(gg \to H)$ is computed averaging over incoming and summing over outgoing spin and color:

$$\sigma_{\rm off} = \frac{1}{J}\frac{1}{256}\mathcal{M}^{\mu\nu}_{ab}\mathcal{M}^{*\mu'\nu'}_{ba}\sum_{\lambda_1}\varepsilon^{\lambda_1}_{\mu}(k_1)\varepsilon^{*\lambda_1}_{\mu'}(k_1)\sum_{\lambda_2}\varepsilon^{\lambda_2}_{\nu}(k_2)\varepsilon^{*\lambda_2}_{\nu'}(k_2)\,d\mathcal{P}, \tag{15}$$

where the flux factor

$$J = 2(k_1\cdot k_2 - \mathbf{k}_1\cdot\mathbf{k}_2) \tag{16}$$

is determined on the surface orthogonal to p_1, p_2 eq. (13), and the phase space is

$$d\mathcal{P} = \frac{2\pi}{m_H^2}\delta\left(\frac{1}{z} - 1 - \frac{|\mathbf{k}_1+\mathbf{k}_2|^2}{m_H^2}\right). \tag{17}$$

Note that the kinematics for a $2 \to 1$ process is fixed, so eq. (15) gives the total cross section and no phase–space integration is needed.

The sums over gluon polarizations are given by

$$\sum_{\lambda_i}\varepsilon^{\lambda_i}_{\mu}(k_i)\varepsilon^{*\lambda_i}_{\nu}(k_i) = 2\frac{\mathbf{k}_i^{\mu}\mathbf{k}_i^{\nu}}{|\mathbf{k_i^2}|}; \quad i=1,2. \tag{18}$$

Here, the virtualities will be parametrized through the dimensionless variables

$$\xi_i \equiv \frac{|\mathbf{k}_i|^2}{m_H^2}. \tag{19}$$

The reduced cross section $\bar{\sigma}$, obtained extracting an overall factor m_H^2,

$$m_H^2\sigma_{\rm off}(gg\to H) \equiv \bar{\sigma}(y_t;\xi_1,\xi_2,\varphi,z), \tag{20}$$

is then a dimensionless function $\bar{\sigma}(y_t;\xi_1,\xi_2,\varphi,z)$ of the parameter y_t eq. (4) and of the kinematic variables ξ_1, ξ_2, the relative angle φ of the two transverse momenta

$$\varphi = \cos^{-1}\left(\frac{\mathbf{k}_1\cdot\mathbf{k}_2}{|\mathbf{k}_1||\mathbf{k}_2|}\right), \tag{21}$$

and

$$z \equiv \frac{m_H^2}{2z_1z_2p_1\cdot p_2} = \frac{m_H^2}{2\,(k_1\cdot k_2 - \mathbf{k_1}\cdot\mathbf{k_2})}. \tag{22}$$

Note that, in the collinear limit $\mathbf{k}_1$, $\mathbf{k}_2 \to 0$, z eq. (22) reduces to τ eq. (3).

- The reduced cross section is averaged over φ, and its dependence on z eq. (22) is Mellin-transformed:

$$\bar{\sigma}(N,\xi_1,\xi_2) = \int_0^1 dz\, z^{N-1} \int_0^{2\pi} \frac{d\varphi}{2\pi}\, \bar{\sigma}(y_t;\xi_1,\xi_2,\varphi,z). \tag{23}$$

- The dependence on ξ_i is also Mellin-transformed, and the coefficient of the collinear pole in M_1, M_2 is extracted:

$$h(N,M_1,M_2) = M_1 M_2 \int_0^\infty d\xi_1 \int_0^\infty d\xi_2\, \xi_1^{M_1-1} \xi_2^{M_2-1} \bar{\sigma}(N,\xi_1,\xi_2). \tag{24}$$

  Note that the integral in eq. (24) has a simple pole in both $M_1 = 0$ and $M_2 = 0$. The residue of this pole is the usual hard coefficient function as determined in collinear factorization, which is thus $C(N) = h(N,0,0)$.

- The leading singularities of the hard coefficient function eq. (12) are obtained by expanding in powers of α_s at fixed α_s/N the function obtained when M_1 and M_2 in eq. (24) are identified with the leading singularities of the largest eigenvalue of the singlet anomalous dimension matrix, namely

$$m_H^2 \sigma_0(y_t) C(\alpha_s(m_H^2),N,y_t) = h\left(N, \gamma_s\left(\frac{\alpha_s}{N}\right), \gamma_s\left(\frac{\alpha_s}{N}\right)\right)\left[1 + O\left(\alpha_s\right)\right]. \tag{25}$$

  Here, γ_s is the leading order term in the expansion of the large eigenvalue γ^+ of the singlet anomalous dimension matrix in powers of α_s at fixed α_s/N:

$$\gamma^+(\alpha_s,N) = \gamma_s\left(\frac{\alpha_s}{N}\right) + \gamma_{ss}\left(\frac{\alpha_s}{N}\right) + \ldots, \tag{26}$$

with [15]

$$\gamma_s\left(\frac{\alpha_s}{N}\right) = \sum_{n=1}^{\infty} c_n \left(\frac{C_A \alpha_s}{\pi N}\right)^n; \quad c_n = 1,0,0,2\zeta(3),\ldots, \tag{27}$$

where $C_A = 3$.

So far, this procedure has been used to determine the leading nontrivial singularities to the hard coefficients for a small number of processes: heavy quark photo– and electro–production [12], deep–inelastic scattering [16], heavy quark hadroproduction [17,18], and Higgs production in the infinite m_t limit [13].

2.2 Cross section for Higgs production from two off-shell gluons

The leading–order amplitude for the production of a Higgs in the fusion of two off–shell gluons with momenta k_1 and k_2 and color a,b is given by the single triangle diagram, and it is equal to

$$\begin{aligned}\mathcal{M}_{ab}^{\mu\nu} &= 4i\,\delta^{ab}\,\frac{g_s^2 m_t^2}{v}\left[\frac{k_2^\mu k_1^\nu}{m_H^2} A_1(\xi_1,\xi_2;y_t) - g^{\mu\nu} A_2(\xi_1,\xi_2;y_t)\right.\\ &\left. + \left(\frac{k_1\cdot k_2}{m_H^2} A_1(\xi_1,\xi_2;y_t) - A_2(\xi_1,\xi_2;y_t)\right)\frac{k_1\cdot k_2 k_1^\mu k_2^\nu - k_1^2 k_2^\mu k_2^\nu - k_2^2 k_1^\mu k_1^\nu}{k_1^2 k_2^2}\right], \end{aligned} \tag{28}$$

where the strong coupling is $\alpha_s = \frac{g_s^2}{4\pi}$ and the top Yukawa coupling is given by $h_t = \frac{m_t}{v}$ in terms of the Higgs vacuum-expectation value v, related to the Fermi coupling by $G_F = \frac{1}{\sqrt{2}v^2}$. The dimensionless form factors $A_1(\xi_1, \xi_2; y_t)$ and $A_2(\xi_1, \xi_2; y_t)$ have been computed in ref. [11]; their explicit expression is given in the appendix. They were subsequently rederived in Ref. [19], where an expression for the Higgs production cross section from the fusion of two off-shell gluons was also determined, but was not used to obtain the high energy corrections to perturbative coefficient functions.

The spin- and colour-averaged reduced cross section eq. (20) is then found using eq. (15), with the phase space eq. (17). We get

$$\bar{\sigma}(y_t; \xi_1, \xi_2, \varphi, z) = 8\sqrt{2}\pi^3 \alpha_s^2 G_F m_H^2 \frac{y_t^2}{\xi_1 \xi_2} \left| \frac{1}{2z} A_1 - A_2 \right|^2 \delta\left(\frac{1}{z} - 1 - \xi_1 - \xi_2 - \sqrt{\xi_1 \xi_2} \cos\varphi \right). \quad (29)$$

Because of the momentum–conserving delta, the Mellin transform with respect to z is trivial, and the reduced cross section eq. (23) is given by

$$\begin{aligned} \bar{\sigma}(N, \xi_1, \xi_2) = 8\sqrt{2}\pi^3 \alpha_s^2 G_F m_H^2 y_t^2 \int_0^{2\pi} \frac{d\varphi}{2\pi} \frac{1}{(1+\xi_1+\xi_2)^N} \frac{1}{(1+\sqrt{\alpha}\cos\varphi)^N} \\ \left[\left(|A_1|^2 \cos^2\varphi + \xi_1 \xi_2 |A_3|^2 \right) + \frac{1}{\sqrt{\xi_1 \xi_2}} \left[|A_1|^2 (1+\xi_1+\xi_2) - (A_1^* A_2 + A_1 A_2^*) \right] \cos\varphi \right], \end{aligned} \quad (30)$$

where we have defined the dimensionless variable

$$\alpha \equiv \frac{4\xi_1 \xi_2}{(1+\xi_1+\xi_2)^2}. \quad (31)$$

The three form factors A_i are independent of φ, so all the angular integrals can be performed in terms of hypergeometric functions, with the result

$$\begin{aligned} \bar{\sigma}(N, \xi_1, \xi_2) = 8\sqrt{2}\pi^3 \alpha_s^2 G_F m_H^2 y_t^2 \frac{1}{(1+\xi_1+\xi_2)^N} \Bigg\{ \frac{|A_1|^2}{2} \Big({}_2F_1(\frac{N}{2}, \frac{N+1}{2}, 2, \alpha) \\ + \frac{\alpha}{4} N(N+1) {}_2F_1(\frac{N+2}{2}, \frac{N+3}{2}, 3, \alpha) \Big) + \xi_1 \xi_2 |A_3|^2 {}_2F_1(\frac{N}{2}, \frac{N+1}{2}, 1, \alpha) \\ - N \left[|A_1|^2 (1+\xi_1+\xi_2) - (A_1^* A_2 + A_1 A_2^*) \right] \frac{1}{1+\xi_1+\xi_2} {}_2F_1(\frac{N+1}{2}, \frac{N+2}{2}, 2, \alpha) \Bigg\}. \end{aligned} \quad (32)$$

In the limit $m_t \to \infty$, using the behaviour of the form factors eq. (60) the term in square brackets in eq. (32) as well as the term proportional to A_3 are seen to vanish. The remaining terms, proportional to A_1, give the result in the pointlike limit. The reduced cross section in this limit was already derived in ref. [13] (see eq. (9) of that reference): our result differs from that of ref. [13], though the disagreement is by terms of relative $O(N)$, hence it is immaterial for the subsequent determination of the leading singularities of the hard coefficient function.

2.3 High energy behaviour

The leading singularities of the coefficient function can now be determined from the Mellin transform $h(N, M_1, M_2)$ eq. (24) of the reduced cross section eq. (32), letting $M_1 = M_2 = \gamma_s(\alpha_s/N)$ according to eq. (25), and expanding in powers of α_s (i.e. effectively in powers of M_1, M_2) and then in powers of N about $N = 0$. In the pointlike case ($m_t \to \infty$) the Mellin integral eq. (24) diverges for all M_1, M_2 when $N = 0$, and it only has a region of convergence when $N > 0$. As a consequence, the function $h(N, M_1, M_2)$ eq. (24) has singularities in the M plane whose location depends on the value of N, namely, simple poles of the form $\frac{1}{N-M_1-M_2}$: the expansion in powers of M_i has finite radius of convergence $M_i < N$, leading to an expansion in powers of $\frac{M_i}{N}$ and thus double poles when $M_i = \gamma_s$.

In the resolved case (finite m_t) we expect the Mellin integral to converge when $N = 0$ at least for $0 < M_i < M_0$, for some real positive M_0. We can then set $N = 0$, and obtain the leading singularities of the coefficient function from the expansion in powers of M of $h(0, M, M)$, letting $M = \gamma_s$. This turns out to be indeed the case: when $N = 0$, $\bar{\sigma}(N, \xi_1, \xi_2)$ only depends on ξ_1, ξ_2 through the form factors, and the combination of form factors which appear in $\bar{\sigma}$ eq. (32) is regular when ξ_1, $\xi_2 \to 0$ (see eq. (63)), while it vanishes when ξ_1, $\xi_2 \to \infty$ (see eq. (64)). Hence, we can let $N = 0$ in $\bar{\sigma}$, and get

$$\begin{aligned} h(0, M_1, M_2) &= 8\sqrt{2}\pi^3 \alpha_s^2 G_F m_H^2 y_t^2 \\ &\times M_1 M_2 \int_0^{+\infty} d\xi_1 \xi_1^{M_1-1} \int_0^{+\infty} d\xi_2 \xi_2^{M_2-1} \left[\frac{1}{2}|A_1|^2 + \xi_1 \xi_2 |A_3|^2 \right]. \end{aligned} \tag{33}$$

Because the term in square brackets in eq. (33) tends to a constant as ξ_1, $\xi_2 \to 0$, the integrals in eq. (33) have an isolated simple pole in M_1 and M_2, and thus the Taylor expansion of $h(N, M_1, M_2)$ has a finite radius of convergence. We can then determine the Taylor coefficients by expanding the integrand of eq. (33) and integrating term by term. It follows from eqs. (25-27) that knowledge of the coefficients up to k-th order in both M_1 and M_2 is necessary and sufficient to determine the leading singularity of the coefficient function up to order α_s^k.

Let us now determine the leading singularities of first three coefficients of the expansion of the coefficient function eq. (8). The constant term determines the leading–order result σ_0 eq. (8):

$$m_H^2 \sigma_0(y_t) = h(0, 0, 0). \tag{34}$$

Using the on-shell limit of the form factors (see eq. (63) of the appendix) in eq. (33) we reproduce the well-known result eq. (10).

The next-to-leading order term $C^{(1)}(N, y_t)$ is determined by noting that

$$\begin{aligned} h(0, M, 0) &= 4\sqrt{2}\pi^3 \alpha_s^2 G_F m_H^2 y_t^2 M \int_0^{+\infty} d\xi \, \xi^{M-1} |A_1(\xi, 0)|^2 \\ &= h(0, 0, 0) - 8\sqrt{2}\pi^3 \alpha_s^2 G_F m_H^2 y_t^2 M \int_0^{+\infty} d\xi \ln \xi \frac{d|A_1(\xi, 0)|^2}{d\xi} + O(M^2). \end{aligned} \tag{35}$$

m_H	$\mathcal{C}^{(1)}(y_t)$	$\mathcal{C}^{(2)}(y_t)$
110	5.0447	16.2570
120	4.6873	14.5133
130	4.3568	13.0155
140	4.0490	11.7196
150	3.7607	10.5919
160	3.4890	9.6058
170	3.2318	8.7406
180	2.9872	7.9794
190	2.7536	7.3085
200	2.5296	6.7166
210	2.3140	6.1946
220	2.1057	5.7346
230	1.9037	5.3303
240	1.7072	4.9761
250	1.5151	4.6677
260	1.3267	4.4013
270	1.1409	4.1738
280	0.9568	3.9828
290	0.7731	3.8268
300	0.5884	3.7049

Table 1: Values of the coefficients eq. (36) and eq. (38) of the $O(\alpha_s/N)$ and $O((\alpha_s/N)^2)$ of the leading singularities of the coefficient function $C(\alpha_s(m_H^2); N, y_t)$ eq. (12).

Equations (25-27) then immediately imply that

$$C^{(1)}(N, y_t) = \mathcal{C}^{(1)}(y_t)\frac{C_A}{N}\left[1 + O(N)\right],$$
$$\mathcal{C}^{(1)} = -\frac{2(8\pi^2)^2}{\left|\left(1 - \frac{1}{4}(1-4y_t)s_0(y_t)^2\right)\right|^2}\int_0^{+\infty} d\xi \ln\xi \frac{d|A_1(\xi,0)|^2}{d\xi}. \tag{36}$$

The value of the coefficient $\mathcal{C}^{(1)}$, determined from a numerical evaluation of the integral in eq. (36), is tabulated in table 1 as a function of the Higgs mass. Upon inverse Mellin transformation, one finds that

$$\lim_{\tau\to 0} C^{(1)}(\tau, y_t) = C_A \mathcal{C}^{(1)}(y_t). \tag{37}$$

The values given in table 1 are indeed found to be in perfect agreement with a numerical evaluation of the small τ limit of the full NLO coefficient function $C^{(1)}(\tau, y_t)$ [4], for which we have used the form given in ref. [20].

Turning finally to the determination of the hitherto unknown NNLO leading singularity, we

evaluate the $O(M^2)$ terms in the expansion eq. (35): by using again eqs. (25-27) we find

$$
\begin{aligned}
C^{(2)}(N,y_t) &= \mathcal{C}^{(2)}(y_t)\frac{C_A^2}{N^2}\left[1+O(N)\right] \\
\mathcal{C}^{(2)}(y_t) &= -\frac{(8\pi^2)^2}{\left|\left(1-\frac{1}{4}(1-4y_t)s_0(y_t)^2\right)\right|^2}\left\{\int_0^{+\infty} d\xi \ln^2\xi \frac{d|A_1(\xi,0)|^2}{d\xi}\right. \\
&\left. -\int_0^{+\infty} d\xi_1 \int_0^{+\infty} d\xi_2 \left[\ln\xi_1 \ln\xi_2 \frac{\partial^2 |A_1(\xi_1,\xi_2)|^2}{\partial\xi_1\partial\xi_2} + 2|A_3(\xi_1,\xi_2)|^2\right]\right\}.
\end{aligned}
\tag{38}
$$

The value of the NNLO coefficient $\mathcal{C}^{(2)}(y_t)$ obtained from numerical evaluation of the integrals in eq. (38) is also tabulated in table 1. This is the main result of the present paper.

3 Improvement of the NLO and NNLO cross sections

Knowledge of the leading small τ behaviour of the exact coefficient function $C(\alpha_s(m_H^2);\tau,y_t)$ eq. (8) can be used to improve its determination. Indeed, as discussed in section 1, we expect the pointlike ($m_t \to \infty$) approximation to be quite accurate at large τ, whereas we know that it must break down as $\tau \to 0$. Specifically, the small τ behaviour of the coefficient function is dominated by the highest rightmost singularity in $C(\alpha_s(m_H^2);N,y_t)$ eq. (12), which for the exact result is a k-th order pole but becomes a $2k$-th order pole in the pointlike approximation. Hence the pointlike approximation displays a spurious stronger growth eq. (1) at small enough τ.

Having determined the exact small τ behaviour up to NNLO, we can improve the approximate pointlike determination of the coefficient function by subtracting its spurious small τ growth and replacing it with the exact behaviour. We discuss first the NLO case, where the full exact result is known, and then turn to the NNLO where only the $m_t \to \infty$ result is available.

3.1 NLO results

At NLO the small τ behaviour of the coefficient function in the pointlike approximation is dominated by a double pole, whereas it is given by the simple pole eq. (36) in the exact case. This corresponds to an exact NLO contribution $C^{(1)}(\tau,y_t)$ which tends to a constant at small τ, whereas the pointlike approximation to it grows as $\ln\tau$:

$$
C^{(1)}(\tau,\infty) = d^{(1)}_{\rm point}(\tau) + O(\tau); \quad d^{(1)}_{\rm point}(\tau) = c^1{}_2 \ln\tau + c^1{}_1 \tag{39}
$$

$$
C^{(1)}(\tau,y_t) = d^{(1)}_{\rm ex}(\tau,y_t) + O(\tau); \quad d^{(1)}_{\rm ex}(\tau,y_t) = 3\mathcal{C}^{(1)}(y_t), \tag{40}
$$

where $\mathcal{C}^{(1)}(y_t)$ is tabulated in table 1, while from Refs. [4, 6, 7] we get

$$
c^1{}_2 = -6; \quad c^1{}_1 = -\frac{11}{2}. \tag{41}
$$

The NLO term $C^{(1)}(\tau,y_t)$ eq. (8) is plotted as a function of τ in fig. 1, both in the pointlike ($m_t \to \infty$) approximation, and in its exact form computed with increasing values of the Higgs

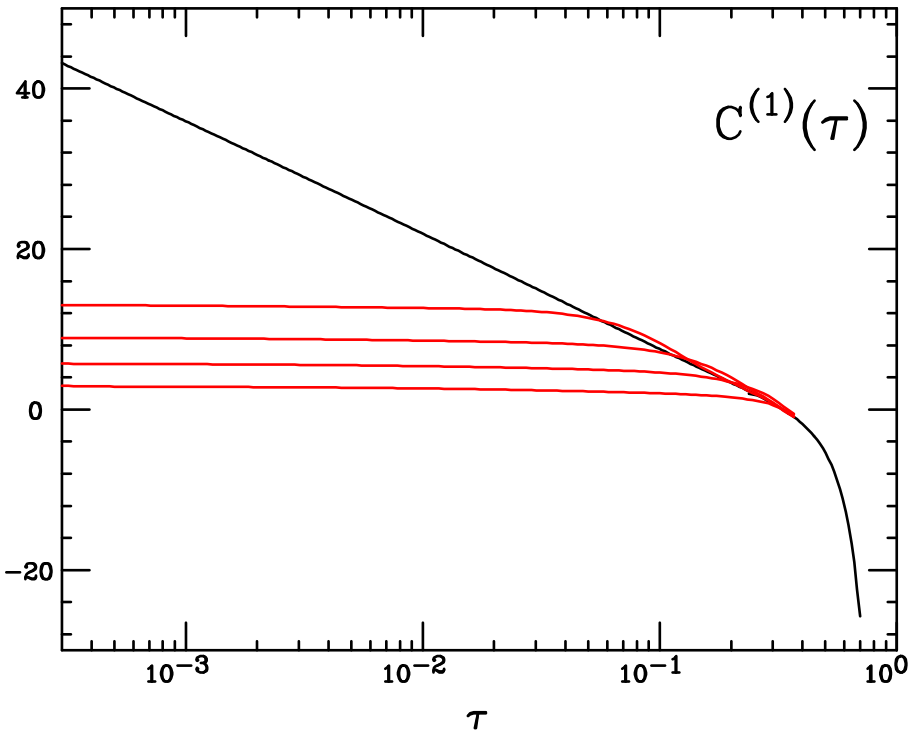

Figure 1: The hard coefficient $C^{(1)}(\tau, y_t)$ eq. (9) (parton–level coefficient function normalized to the Born result) plotted as a function of τ. The curves from top to bottom on the left correspond to $m_t = \infty$ (black), and to $m_t = 170.9$ GeV (red), with $m_H = 130,\ 180,\ 230,\ 280$ GeV.

mass, i.e. decreasing values of y_t. It is apparent that the pointlike approximation is very accurate, up to the point where the spurious logarithmic growth eq. (39) sets in.

We can construct an approximation to $C^{(1)}(\tau, y_t)$ by combining the pointlike approximation with the exact small τ behaviour:

$$C^{(1),\mathrm{app.}}(\tau, y_t) \approx C^{(1)}(\tau, \infty) + \left[d^{(1)}_{\mathrm{ex}}(\tau, y_t) - d^{(1)}_{\mathrm{point}}(\tau) \right] T(\tau) \tag{42}$$

where $d^{(1)}_{\mathrm{ex}}(\tau, y_t)$ and $d^{(1)}_{\mathrm{point}}(\tau)$ are defined as in eq. (40) and eq. (39) respectively, while $T(\tau)$ is an interpolating function, which we may introduce in order to tune the point where the small τ behaviour given by $d^{(1)}_{\mathrm{ex}}(\tau, y_t)$ sets in. Clearly, as $\tau \to 0$ the approximation eq. (42) reproduces the exact small τ behaviour of the exact coefficient function eq. (40), provided only the interpolating function $\lim_{\tau\to 0} T(\tau) = 1$. Furthermore, as discussed in section 1, the behaviour of the coefficient function $C^{(1)}(\tau, y_t)$ as $\tau \to 1$ is to all orders controlled by soft gluon radiation, which leads to contributions to $C^{(1)}(\tau, y_t)$ which do not depend on y_t and diverge as $\tau \to 1$. Hence, the pointlike approximation is exact as $\tau \to 1$. Because the functions $d^{(1)}_{\mathrm{ex}}(\tau, y_t)$ and $d^{(1)}_{\mathrm{point}}(\tau)$ are regular as $\tau \to 1$, this exact behaviour is also reproduced by the approximation eq. (42), provided only $\lim_{\tau\to 1} T(\tau)$ is finite. Hence, $C^{(1),\mathrm{app.}}(\tau, y_t)$ reproduces the exact $C^{(1)}(\tau, y_t)$ as $\tau \to 0$ up to terms

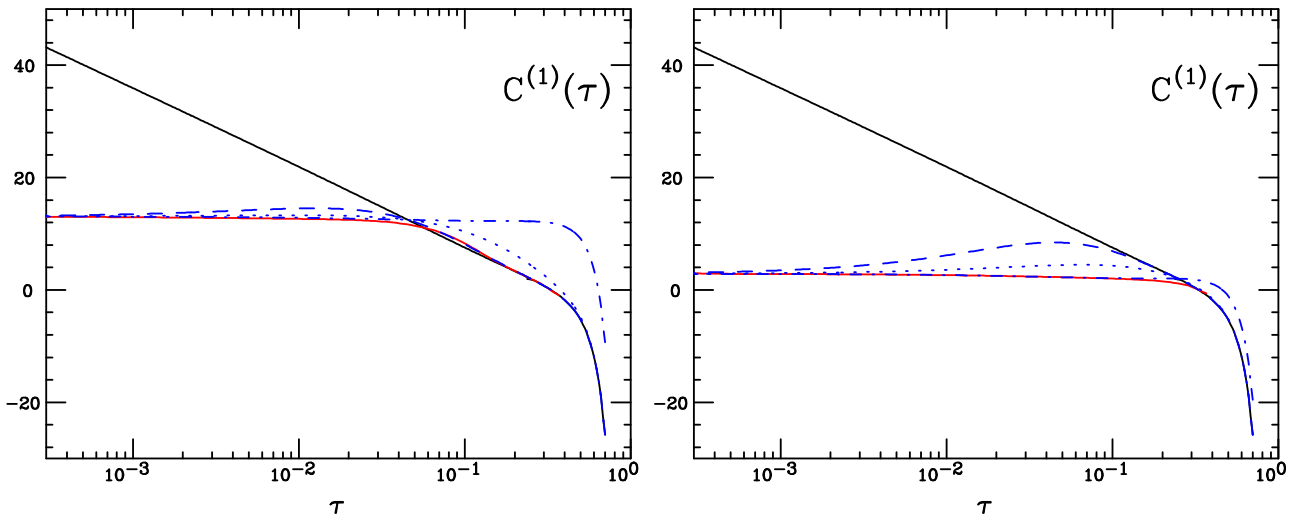

Figure 2: The hard coefficient $C^{(1)}(\tau, y_t)$ eq. (9) with $m_H = 130$ GeV (left) and $m_H = 280$ GeV (right). The solid curves correspond to $m_t = \infty$ (black) and $m_t = 170.9$ GeV (red), (same as fig. 1). The three blue curves correspond to the approximation eq. (42,43), with $k = 0$ (dot-dashed), $k = 5$ (dotted), $k = 20$ (dashed).

that vanish as $\tau \to 0$ and as $\tau \to 1$ up to terms that are nonsingular as $\tau \to 1$, even when $T(\tau) = 1$.

Nevertheless, we may also choose $T(\tau)$ in such a way that $T(1) = 0$ (while $T(0) = 1$ always), so that $C^{(1)}(\tau, y_t)$ agrees with the pointlike approximation $C^{(1)}(\tau, \infty)$ in some neighborhood of $\tau = 1$. For instance, we can let

$$T(\tau) = (1 - \tau)^k, \tag{43}$$

with k real and positive, so that the first k orders of the Taylor expansion about $\tau = 1$ of $C^{(1),\text{app.}}(\tau, y_t)$ and the pointlike approximation coincide. By varying the value of k, we can choose the matching point τ_0, such that $C^{(1),\text{app.}}(\tau, y_t)$ only differs significantly from the pointlike approximation if $\tau < \tau_0$: a larger value of k leads to a smaller value of τ_0.

In fig. 2 we compare the approximate NLO term eq. (42) to the exact and pointlike results, for two different values of y_t, with $T(\tau)$ given by eq. (43) and a choice of k which leads to different values of the matching between approximate and pointlike curves. It appears that an optimal matching is obtained by choosing k in such a way that the approximation eq. (42) matches the pointlike result close to the point where the logarithmic growth of the latter intersects the asymptotic constant value of the exact result. Note that this optimal matching could be determined without knowledge of the exact result. With this choice, the approximation eq. (42) differs from the exact result for the NLO contribution to the partonic cross section by less than 5% for all values of τ.

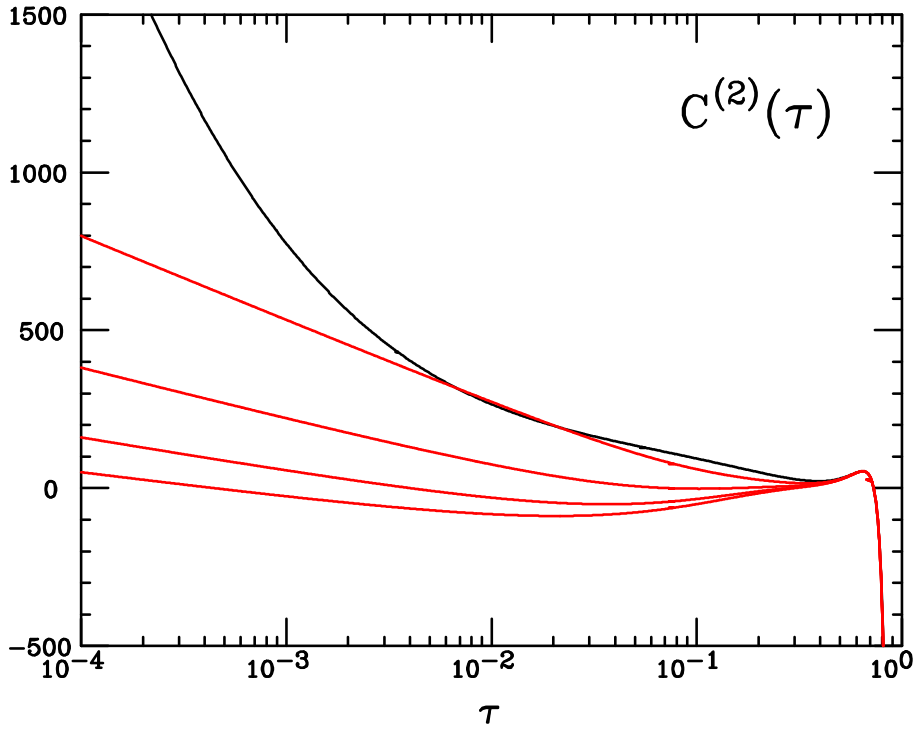

Figure 3: The hard coefficient $C^{(2)}(\tau, y_t)$ eq. (9) (parton–level coefficient function normalized to the Born result) plotted as a function of τ. The curves from top to bottom on the left correspond to $m_t = \infty$ (black), and to the approximation eq. (47) with $T(\tau)$ eq. (43) and $k = 5$, and $m_t = 170.9$ GeV (red), with $m_H = 130,\ 180,\ 230,\ 280$ GeV.

3.2 NNLO and beyond

At NNLO, the pointlike approximation to the coefficient function has a quadruple pole at $N = 0$, corresponding to a $\ln^3 \tau$ rise, while the exact result only has a double pole, and thus it rises linearly with $\ln \tau$:

$$C^{(2)}(\tau, \infty) = d^{(2)}_{\rm point}(\tau) + O\left(\tau^0\right); \quad d^{(2)}_{\rm point}(\tau) = {c^2}_4 \ln^3 \tau + {c^2}_3 \ln^2 \tau + {c^2}_2 \ln \tau \tag{44}$$

$$C^{(2)}(\tau, y_t) = d^{(2)}_{\rm ex}(\tau, y_t) + O\left(\tau^0\right); \quad d^{(2)}_{\rm ex}(\tau, y_t) = -9\, \mathcal{C}^{(2)}(y_t) \ln \tau, \tag{45}$$

where $\mathcal{C}^{(2)}(y_t)$ is tabulated in table 1, while from Ref. [8] we get

$${c^2}_4 = -6; \quad {c^2}_3 = -\frac{231}{4} + n_f \frac{17}{18}; \quad {c^2}_2 = \left(-\frac{2333}{8} + 3\pi^2\right) + n_f \frac{641}{108}, \tag{46}$$

where n_f the number of flavors.

At this order, the exact form of $C^{(2)}(\tau, y_t)$ is not known. However, analogously to the NLO case, we construct an approximation to it based on its determination [8] in the pointlike limit,

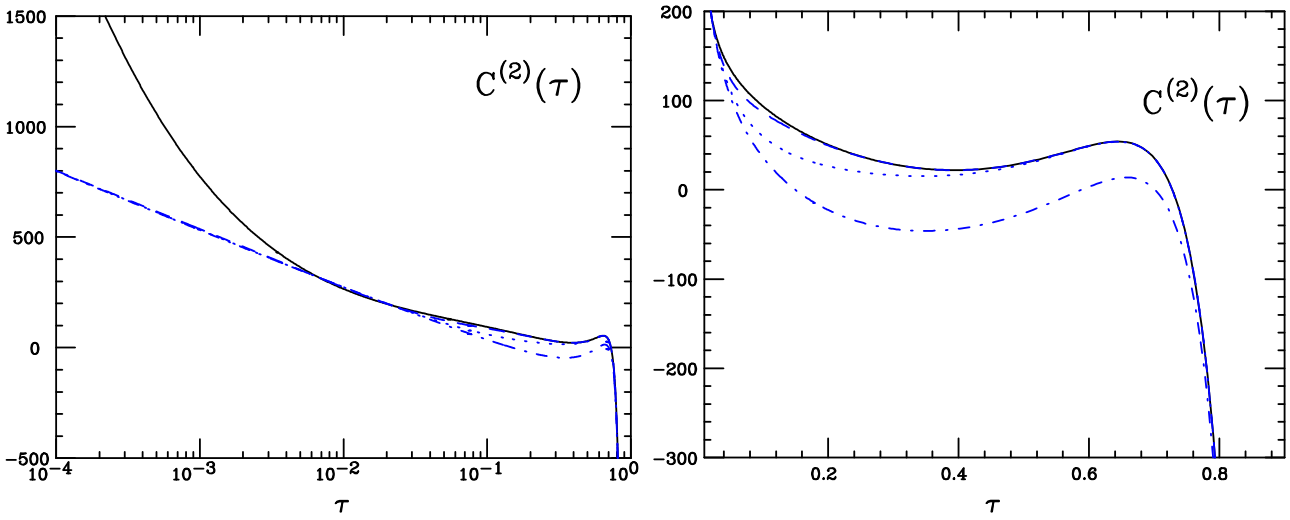

Figure 4: The hard coefficient $C^{(2)}(\tau, y_t)$ eq. (9) with $m_H = 130$ GeV, plotted versus τ on a logarithmic (left) or linear (right) scale. The solid black curve corresponds to $m_t = \infty$ (black, same as fig. 3)), and the three blue curves are the approximation eq. (47) with $m_t = 170.9$ GeV and $T(\tau)$ eq. (43) with and $k = 0$ (dot-dashed), $k = 5$ (dotted, same as fig. 3), $k = 20$ (dashed).

combined with the exact small τ behaviour eq. (38):

$$C^{(2),\text{app.}}(\tau, y_t) \approx C^{(2)}(\tau, \infty) + \left[d^{(2)}_{\text{ex}}(\tau, y_t) - d^{(2)}_{\text{point}}(\tau)\right] T(\tau) \tag{47}$$

with $d^{(2)}_{\text{ex}}(\tau, y_t)$ and $d^{(2)}_{\text{point}}(\tau)$ defined in eq. (45) and eq. (44) respectively, and $T(\tau)$ an interpolating function as discussed in section 3.1. Note that as $\tau \to 0$ the approximation eq. (47) only reproduces the exact result up to a constant, whereas at NLO the approximation eq. (42) reproduces the exact result up to terms which vanish at least as $O(\tau)$.

The approximation to the exact result $C^{(2),\text{app.}}(\tau, y_t)$, computed using $\mathcal{C}^{(2)}$ from table 1 with four different values of the Higgs mass, and taking $T(\tau)$ eq. (43) with $k = 5$ is compared in fig. 3 to the pointlike approximation $C^{(2),\text{app.}}(\tau, y_t)$ of ref. [8] (with $n_f = 5$). In figures 4-5 we further compare the results obtained with different choices of the matching function $T(\tau)$ eq. (43), and the same two values of the Higgs mass used to produce figs. 2-3 at NLO.

At this order, the contribution from the leading small τ logs to the pointlike $C^{(2),\text{app.}}(\tau, \infty)$ is sizable even for large τ. Indeed, figs. 4-5 show that the behaviour of $C^{(2)}$ around its local maximum at $\tau \approx 0.65$ receives a sizable contribution from the $\ln \tau$ rise and $\ln^2 \tau$ drop eq. (44). If these are removed by using eqs. (47,43) with $k = 0$, the shape of $C^{(2)}$ around the maximum is affected significantly, but if the matching is moved to smaller τ by choosing $k \gtrsim 5$ the maximum is reproduced. Hence, whereas we can still obtain a rather smooth matching at any desired value of τ the choice of the optimal value of τ is not obvious. In particular, matching at a value of τ

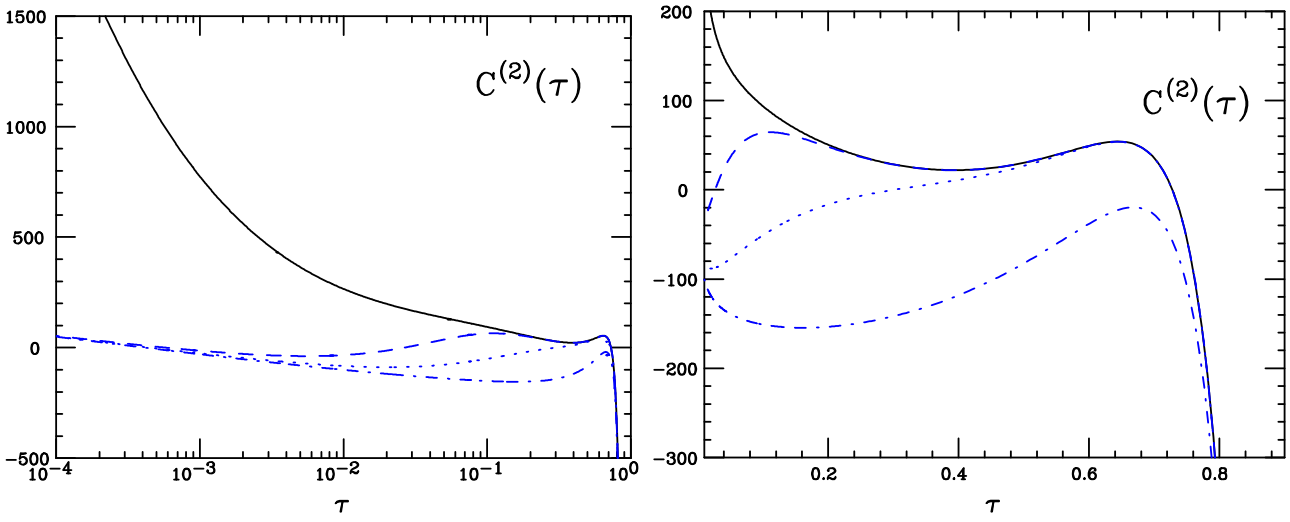

Figure 5: Same as fig. 4, but now with $m_H = 280$ GeV.

where the contribution of the asymptotically spurious $\ln^2 \tau$ becomes significant leads to rather large values of the matching point $\tau \gtrsim 0.6$. Anyway, it is clear that the pointlike approximation breaks down for $\tau \lesssim 0.1$.

Contributions beyond NNLO in the expansion of $h(N, \gamma_s, \gamma_s)$ eq. (25) in powers of $\frac{\alpha_s}{N}$ can be determined by pursuing the expansion of $h(0, M, M)$ eq. (33) in powers of M, and determining numerically the ensuing integrals, which have the form of eqs. (36,38), but with higher order powers of $\ln \xi_1$, $\ln \xi_2$. The series of contributions to the coefficient function eq. (8) thus obtained has a finite radius of convergence in N–Mellin space, dictated by the location of the rightmost singularity in γ_s, and thus in τ space it converges for all $0 < \tau \leq 1$ [22]. Therefore, its resummation can be accomplished to arbitrary accuracy by computation of a finite number of terms. This resummation, however, induces spurious singularities in the N–space coefficient function, which can be removed by the inclusion of a suitable class of formally subleading running-coupling corrections, as recently shown in Ref. [23].

3.3 K factors

The accuracy of the various approximations at the level of hadronic observables clearly depends on the individual process. For the total inclusive cross section eq. (5), as is well known, the pointlike approximation is actually very good, and thus the impact of the improvement eq. (42)

	$\kappa^{\rm NLO}$	$\kappa^{\rm NNLO}$
$m_H = 130$ GeV		
pointlike	36.69	658
exact	36.58	n.a.
appr., $k = 5$	37.64	648
appr., $k = 20$	36.66	655
$m_H = 280$ GeV		
pointlike	38.08	716
exact	37.47	n.a.
appr., $k = 2$	37.97	670
appr., $k = 5$	37.73	693

Table 2: The NLO and NNLO contributions to the K factor eq. (48), computed with center-of-mass energy $s = 14$ TeV, and $m_t \to \infty$, denoted with pointlike, or $m_t = 170.9$ GeV, denoted with exact or approximate. The approximate result uses eqs. (42,47), with $T(\tau)$ eq. (43) and the value of k given in the table. The MRST2002 [21] gluon distribution has been used.

is moderate. To give a quantitative assessment, we define a K factor by letting:

$$\begin{aligned}
\sigma_{gg}(\tau_h; y_t, m_H^2) &= \sigma^0_{gg}(\tau_h; y_t, m_H^2) K(\tau_h; y_t, m_H^2) \\
K(\tau_h; y_t, m_H^2) &= 1 + \frac{\alpha_s(m_H^2)}{\pi} \kappa^{\rm NLO}(\tau_h; y_t, m_H^2) + \left(\frac{\alpha_s(m_H^2)}{\pi}\right)^2 \kappa^{\rm NNLO}(\tau_h; y_t, m_H^2) \\
&\quad + O\left(\alpha_s^3(m_H^2)\right), \qquad (48)
\end{aligned}$$

where σ^0_{gg} is the leading–order form of the contribution eq. (5) of the gluon–gluon channel to total hadronic cross section. The value of the NLO and NNLO contributions to the K factors, determined using the MRST2002 [21] gluon distribution in eq. (5) are given in table 2 at LHC energies for two values of the Higgs mass, both in the pointlike, exact and approximate (eq. (42) and eq. (47)) cases.

At NLO with $m_H = 130$ GeV ("light"), the pointlike approximation to $\kappa^{\rm NLO}$ deviates by 0.3% from the exact result, and even with $m_H = 280$ GeV ("heavy") it only deviates by 1.6%. It should be kept in mind, however, that $\kappa^{\rm NLO}$ itself is quite large: for $\alpha_s \approx 0.1$, it amounts to a $\sim 100\%$ contribution to the K factor eq. (48). Hence, the error made using the pointlike approximation is between the per mille and the per cent level, and thus not entirely negligible in a precision analysis.

Using the approximation eqs. (42-43) with the values $k = 20$ for light Higgs and $k = 5$ for heavy Higgs, which are seen from fig. 2 to give good matching, the deviation can be reduced to 0.2% and 0.7% respectively, and even more accurate results could be obtained by an optimization of the matching. However, a poor choice of the matching (such as $k = 5$ for light Higgs or $k = 2$ for heavy Higgs) can lead to a result at the hadronic level which is actually closer to the pointlike approximation, or even worse than it. It is clear that at the partonic level the small τ behaviour eq. (39) accounts for most of the discrepancy between the exact and pointlike results, and even

the determination of a hadronic observable which depends very little on the parton-level small τ behaviour can be improved very substantially for values of τ_H relevant for LHC by using the approximation eq. (42).

The NNLO contribution $\kappa^{\rm NNLO}$ is not known. Its values computed in the pointlike approximation, or with the approximation eqs. (47,43) and different choices of k are shown in table 2. Even at the inclusive hadronic level, now the size of the NNLO contribution can change up to about $5-10\%$ if the matching is performed at large τ. Furthermore, $\kappa^{\rm NNLO}$ is also quite large: with $\alpha_s \approx 0.1$, it amounts to a $\sim 50\%$ correction to the leading order, and thus to a further $\sim 25\%$ correction to the K factor. Therefore, the impact of the pointlike approximation at NNLO is up to several per cent of the total K factor, rather larger that the impact of the pointlike approximation at NLO, and comparable to uncertainties which are currently discussed in precision studies at NNLO.

4 Outlook

In this paper we have determined the leading high energy (i.e. small $\tau = \frac{m_H^2}{\hat{s}}$) singularities of the cross section for Higgs production in gluon–gluon fusion to all orders in the strong coupling, by providing an expression (eq. (33)) whence the coefficients of these singularities can be obtained by Taylor expanding and computing a double integral. We have given explicit numerical expressions for these coefficients up to NNLO.

The high energy behaviour of this cross section is different according to whether it is determined with finite m_t or with $m_t \to \infty$ (pointlike approximation). It turns out that at NLO this different high energy behaviour is responsible for most of the discrepancy between the pointlike approximation and the exact result. As a consequence, an accurate approximation to the exact result can be constructed by combining the pointlike approximation at large τ with the exact small τ behaviour. Some care must be taken in matching, but very accurate results can be obtained by simply choosing the matching point as that where the spurious small τ behaviour of the pointlike behaviour sets in.

At NNLO, where the exact result is not known, the impact of the high energy behaviour turns out to be large even for moderate values of $\tau \sim 0.5$. Hence, an approximation constructed analogously to that which is successful at NLO, namely matching the pointlike limit to the asymptotic exact behaviour at the point where the asymptotically spurious terms become significant, leads to an approximate result which differs significantly from the pointlike approximation for most values of the partonic center-of-mass energy.

The effect of these high energy terms on the total inclusive hadronic cross section remains quite small, because the latter is dominated by the region of low partonic center–of–mass energy, partly due to shape of the gluon parton distributions, which are peaked in the region where the gluons carry a small fraction of the incoming nucleon's energy, and partly because the partonic cross section is peaked in the threshold $\tau \approx 1$ region. Even so, the pointlike determination of the NNLO contribution to the total hadronic cross section can be off by almost 5-10% due to this spurious high energy behaviour, especially for relatively large values of $m_H \gtrsim 200$ GeV. Because the NLO and NNLO corrections to the cross section are quite large, the overall effect of

these terms on the cross section is at the per cent level, and in particular their effect at NNLO is rather larger than at NLO.

A study of the phenomenological implications of these results is thus relevant for a precision determination of the Higgs production cross section.

Acknowledgements: We thank Thomas Binoth and Fabio Maltoni for discussions, and Guido Altarelli for a critical reading of the manuscript. This work was partly supported by the Marie Curie Research and Training network HEPTOOLS under contract MRTN-CT-2006-035505 and by a PRIN2006 grant (Italy). The work of S. Marzani and R.D. Ball was done with the support of the Scottish Universities' Physics Alliance.

A Form factors

The form factors in eq. (28) are given by

$$\begin{aligned} A_1(\xi_1,\xi_2,y_t) &= C_0(\xi_1,\xi_2,y_t)\left[\frac{4y_t}{\Delta_3}(1+\xi_1+\xi_2)-1-\frac{4\xi_1\xi_2}{\Delta_3}+12\frac{\xi_1\xi_2}{\Delta_3^2}(1+\xi_1+\xi_2)\right] \\ &- [B_0(-\xi_2)-B_0(1)]\left[-\frac{2\xi_2}{\Delta_3}+12\frac{\xi_1\xi_2}{\Delta_3^2}(1+\xi_1-\xi_2)\right] \\ &- [B_0(-\xi_1)-B_0(1)]\left[-\frac{2\xi_1}{\Delta_3}+12\frac{\xi_1\xi_2}{\Delta_3^2}(1-\xi_1+\xi_2)\right] \\ &+ \frac{2}{\Delta_3}\frac{1}{(4\pi)^2}(1+\xi_1+\xi_2)\,, \end{aligned} \tag{49}$$

$$\begin{aligned} A_2(\xi_1,\xi_2,y_t) &= C_0(\xi_1,\xi_2,y_t)\left[2y_t-\frac{1}{2}(1+\xi_1+\xi_2)+\frac{2\xi_1\xi_2}{\Delta_3}\right] \\ &+ [B_0(-\xi_2)-B_0(1)]\left[\frac{\xi_2}{\Delta_3}(1-\xi_1+\xi_2)\right] \\ &+ [B_0(-\xi_1)-B_0(1)]\left[\frac{\xi_1}{\Delta_3}(1+\xi_1-\xi_2)\right]+\frac{1}{(4\pi)^2}\,, \end{aligned} \tag{50}$$

with

$$\Delta_3 = 1+\xi_1^2+\xi_2^2-2\xi_1\xi_2+2(\xi_1+\xi_2) = (1+\xi_1+\xi_2)^2-4\xi_1\xi_2\,. \tag{51}$$

It is also convenient to define the form factor

$$A_3(\xi_1,\xi_2,y_t) \equiv \frac{1}{\xi_1\xi_2}\left[\frac{1+\xi_1+\xi_2}{2}A_1-A_2\right]. \tag{52}$$

The scalar integrals B_0 and C_0 are

$$\begin{aligned} B_0(\rho) &= -\frac{1}{8\pi^2}\sqrt{\frac{4y_t-\rho}{\rho}}\,\tan^{-1}\sqrt{\frac{\rho}{4y_t-\rho}}, \quad \text{if} \quad 0<\rho<4y_t\,; \\ B_0(\rho) &= -\frac{1}{16\pi^2}\sqrt{\frac{\rho-4y_t}{\rho}}\,\ln\frac{1+\sqrt{\frac{\rho}{\rho-4y_t}}}{1-\sqrt{\frac{\rho}{\rho-4y_t}}}, \quad \text{if} \quad \rho<0 \text{ or } \rho>4y_t\,; \end{aligned} \tag{53}$$

$$
\begin{aligned}
C_0(\xi_1,\xi_2) \;\equiv\; & \frac{1}{16\pi^2}\frac{1}{\sqrt{\Delta_3}}\Big\{ \ln(1-y_-)\ln\left(\frac{1-y_-\delta_1^+}{1-y_-\delta_1^-}\right) \\
& +\ln(1-x_-)\ln\left(\frac{1-x_-\delta_2^+}{1-x_-\delta_2^-}\right)+\ln(1-z_-)\ln\left(\frac{1-z_-\delta_3^+}{1-z_-\delta_3^-}\right) \\
& +\mathrm{Li}_2(y_+\delta_1^+)+\mathrm{Li}_2(y_-\delta_1^+)-\mathrm{Li}_2(y_+\delta_1^-)-\mathrm{Li}_2(y_-\delta_1^-) \\
& +\mathrm{Li}_2(x_+\delta_2^+)+\mathrm{Li}_2(x_-\delta_2^+)-\mathrm{Li}_2(x_+\delta_2^-)-\mathrm{Li}_2(x_-\delta_2^-) \\
& +\mathrm{Li}_2(z_+\delta_3^+)+\mathrm{Li}_2(z_-\delta_3^+)-\mathrm{Li}_2(z_+\delta_3^-)-\mathrm{Li}_2(z_-\delta_3^-) \quad \Big\}, \qquad (54)
\end{aligned}
$$

where

$$
\delta_1 \equiv \frac{-\xi_1+\xi_2-1}{\sqrt{\Delta_3}}\,, \quad \delta_2 \equiv \frac{\xi_1-\xi_2-1}{\sqrt{\Delta_3}}\,, \quad \delta_3 \equiv \frac{\xi_1+\xi_2+1}{\sqrt{\Delta_3}}\,, \qquad (55)
$$

$$
\delta_i^\pm \equiv \frac{1\pm\delta_i}{2}\,, \qquad (56)
$$

and

$$
\begin{aligned}
x_\pm &\equiv -\frac{\xi_2}{2y_t}\left(1\pm\sqrt{1+\frac{4y_t}{\xi_2}}\right), \\
y_\pm &\equiv -\frac{\xi_1}{2y_t}\left(1\pm\sqrt{1+\frac{4y_t}{\xi_1}}\right), \\
z_\pm &\equiv \frac{1}{2y_t}\left(1\pm i\sqrt{4y_t-1}\right). \qquad (57)
\end{aligned}
$$

In the infinite top mass limit the scalar integrals become

$$
\lim_{y_t\to\infty} B_0(\rho) = \frac{1}{16\pi^2}\left(-2+\frac{\rho}{6y_t}\right)+O\left(\frac{1}{y_t^2}\right), \qquad (58)
$$

$$
\lim_{y_t\to\infty} C_0(\xi_1,\xi_2) = -\frac{1}{32\pi^2 y_t}\left(1+\frac{1-\xi_1-\xi_2}{12y_t}\right)+O\left(\frac{1}{y_t^3}\right), \qquad (59)
$$

so that the form factors reduce to

$$
\lim_{m_t\to\infty} m_t^2 A_1 = m_H^2\frac{1}{48\pi^2}; \qquad \lim_{m_t\to\infty} 4m_t^2 A_2 = m_H^2\frac{\alpha_s}{48\pi^2}\frac{1+\xi_1+\xi_2}{2}. \qquad (60)
$$

These limits also imply that

$$
\lim_{m_t\to\infty} m_t^2 A_3 = 0. \qquad (61)
$$

In the on-shell limit the scalar integrals are

$$
\begin{aligned}
\lim_{\xi_i\to 0} B_0(\xi_i) &= -\frac{1}{8\pi^2}\,, \\
\lim_{\xi_1\to 0} C_0(\xi_1,\xi_2,y_t) &= \frac{1}{32\pi^2}\frac{1}{1+\xi_2}\left(\ln^2\frac{-z_-}{z_+}-\ln^2\frac{-x_-}{x_+}\right), \qquad (62) \\
\lim_{\xi_1,\xi_2\to 0} C_0(\xi_1,\xi_2,y_t) &= \frac{1}{32\pi^2}\left(\ln^2\frac{-z_-}{z_+}\right),
\end{aligned}
$$

so that

$$\begin{aligned} A_1(0,0) &= \frac{1}{8\pi^2} + \frac{1}{32\pi^2}\left(\ln^2\frac{-z_-}{z_+}\right)(4y_t - 1) \\ A_2(0,0) &= \frac{1}{16\pi^2} + \frac{1}{32\pi^2}\left(\ln^2\frac{-z_-}{z_+}\right)\left(2y_t - \frac{1}{2}\right) \end{aligned} \tag{63}$$

The high energy limit of the form factors is trivially determined when $\xi_1 \to \infty$, $\xi_2 \to \infty$ with $\xi_1 \neq \xi_2$:

$$\lim_{\xi_1\to\infty,\xi_2\to\infty} A_1(\xi_1,\xi_2,y_t) = 0;\ \lim_{\xi_1\to\infty,\xi_2\to\infty} A_3(\xi_1,\xi_2,y_t) = 0;\ \lim_{\xi_1\to\infty,\xi_2\to\infty} A_2(\xi_1,\xi_2,y_t) = \frac{1}{(4\pi)^2}. \tag{64}$$

If $\xi_1 \to \infty$, $\xi_2 \to \infty$ with $\xi_1 = \xi_2$ the limit is more subtle. In this case we get

$$\begin{aligned} \lim_{\xi\to\infty} A_1(\xi,\xi,y_t) &= \lim_{\xi\to\infty}\frac{\bar{C}_0(\xi,\xi,y_t)}{4}\sqrt{\xi} - \frac{1}{16\pi^2}\left[\frac{1}{2}\ln\frac{y_t}{\xi} - 1 + \sqrt{4y_t-1}\tan^{-1}\sqrt{\frac{1}{4y_t-1}}\right] \\ &\quad + O\left(\frac{1}{\sqrt{\xi}}\right), \end{aligned} \tag{65}$$

where we have defined

$$\bar{C}_0(\xi_1,\xi_2,y_t) \equiv C_0(\xi_1,\xi_2,y_t)\sqrt{\Delta_3}. \tag{66}$$

However, it turns out that

$$\lim_{\xi\to\infty}\bar{C}_0(\xi,\xi,y_t) = \frac{1}{16\pi^2\sqrt{\xi}}\left[2\ln\frac{y_t}{\xi} - 4 + 4\sqrt{4y_t-1}\tan^{-1}\sqrt{\frac{1}{4y_t-1}}\right] + O\left(\frac{1}{\xi}\right), \tag{67}$$

hence we conclude that eq. (64) holds also when $\xi_1 = \xi_2$.

References

[1] G. P. Salam, Int. J. Mod. Phys. A **21** (2006) 1778.

[2] R. Harlander, Acta Phys. Polon. B **38** (2007) 693.

[3] D. Graudenz, M. Spira and P. M. Zerwas, Phys. Rev. Lett. **70** (1993) 1372.

[4] M. Spira, A. Djouadi, D. Graudenz and P. M. Zerwas, Nucl. Phys. B **453** (1995) 17.

[5] M. Kramer, E. Laenen and M. Spira, Nucl. Phys. B **511** (1998) 523.

[6] A. Djouadi, M. Spira and P. M. Zerwas, Phys. Lett. B **264** (1991) 440.

[7] S. Dawson, Nucl. Phys. B **359** (1991) 283.

[8] C. Anastasiou and K. Melnikov, Nucl. Phys. B **646** (2002) 220; R. V. Harlander and W. B. Kilgore, Phys. Rev. Lett. **88** (2002) 201801; V. Ravindran, J. Smith and W. L. van Neerven, Nucl. Phys. B **665** (2003) 325.

[9] S. Moch and A. Vogt, Phys. Lett. B **631** (2005) 48.

[10] S. Catani, D. de Florian, M. Grazzini and P. Nason, JHEP **0307** (2003) 028.

[11] V. Del Duca, W. Kilgore, C. Oleari, C. Schmidt and D. Zeppenfeld, Nucl. Phys. B **616** (2001) 367.

[12] S. Catani, M. Ciafaloni and F. Hautmann, Phys. Lett. B **242** (1990) 97; S. Catani, M. Ciafaloni and F. Hautmann, Nucl. Phys. B **366** (1991) 135.

[13] F. Hautmann, Phys. Lett. B **535** (2002) 159.

[14] J. R. Ellis, M. K. Gaillard and D. V. Nanopoulos, Nucl. Phys. B **106** (1976) 292; M. A. Shifman, A. I. Vainshtein, M. B. Voloshin and V. I. Zakharov, Sov. J. Nucl. Phys. **30** (1979) 711 [Yad. Fiz. **30** (1979) 1368].

[15] T. Jaroszewicz, Phys. Lett. B **116** (1982) 291.

[16] S. Catani and F. Hautmann, Nucl. Phys. B **427** (1994) 475.

[17] R. D. Ball and R. K. Ellis, JHEP **0105** (2001) 053.

[18] G. Camici and M. Ciafaloni, Nucl. Phys. B **496** (1997) 305 [Erratum-ibid. B **607** (2001) 431].

[19] R. S. Pasechnik, O. V. Teryaev and A. Szczurek, Eur. Phys. J. C **47** (2006) 429.

[20] R. Bonciani, G. Degrassi and A. Vicini, JHEP **0711** (2007) 095.

[21] A. D. Martin, R. G. Roberts, W. J. Stirling and R. S. Thorne, Eur. Phys. J. C **28** (2003) 455.

[22] R. D. Ball and S. Forte, Phys. Lett. B **351** (1995) 313.

[23] R. D. Ball, arXiv:0708.1277 [hep-ph].